

Article

Evaluation of the Multi-Scale Ultra-High Resolution (MUR) Analysis of Lake Surface Temperature

Erik Crosman ^{1,*} , Jorge Vazquez-Cuervo ² and Toshio Michael Chin ²

¹ Department of Atmospheric Sciences, University of Utah, 135 South 1460 East, Rm 819, Salt Lake City, UT 84112, USA

² National Aeronautics and Space Administration Jet Propulsion Laboratory, California Institute of Technology, M/S 300/323 4800 Oak Grove Dr., Pasadena, CA 91109, USA; Jorge.vazquez@jpl.nasa.gov (J.V.-C.); toshio.m.chin@jpl.nasa.gov (T.M.C.)

* Correspondence: erik.crosman@utah.edu; Tel.: +1-801-581-6137

Academic Editor: Xiaofeng Li

Received: 25 May 2017; Accepted: 7 July 2017; Published: 13 July 2017

Abstract: Obtaining accurate and timely lake surface water temperature (LSWT) analyses from satellite remains difficult. Data gaps, cloud contamination, variations in atmospheric profiles of temperature and moisture, and a lack of in situ observations provide challenges for satellite-derived LSWT for climatological analysis or input into geophysical models. In this study, the Multi-scale Ultra-high Resolution (MUR) analysis of LSWT is evaluated between 2007 and 2015 over a small (Lake Oneida), medium (Lake Okeechobee), and large (Lake Michigan) lake. The advantages of the MUR LSWT analyses include daily consistency, high-resolution (~1 km), near-real time production, and multi-platform data synthesis. The MUR LSWT versus in situ measurements for Lake Michigan (Lake Okeechobee) have an overall bias (MUR LSWT-in situ) of -0.20 °C (0.31 °C) and a *RMSE* of 0.86 °C (0.91 °C). The MUR LSWT versus in situ measurements for Lake Oneida have overall large biases (-1.74 °C) and *RMSE* (3.42 °C) due to a lack of available satellite imagery over the lake, but performs better during the less cloudy 15 July–30 September period. The results of this study highlight the importance of calculating validation statistics on a seasonal and annual basis for evaluating satellite-derived LSWT.

Keywords: lake surface temperature; sea surface temperature (SST); surface state; lake modeling; numerical weather prediction; surface analysis

1. Introduction

Lake surface water temperature (LSWT) is an important environmental parameter for understanding lake ecology, biology, and climate change [1–7]. LSWT is also a critical input variable for numerical weather, climate, and hydrological models [8–10]. While extensive climatological data sets and analyses of satellite-derived sea surface temperature (SST) are available and used in a wide range of applications, satellite-derived near real-time LSWT analyses are largely unavailable due to a number of challenges and limited resources [11–13].

Several key factors contribute to the difficulty to provide reliable and consistently accurate near real-time analyses of satellite-derived LSWT: Lake-specific spatially and temporally variable error sources and uncertainties, cloud contamination of thermal retrievals, gaps in coverage due to clouds, and a lack of in situ lake temperature observations. We elaborate on each of these factors below.

Satellite LSWT estimates are generally less accurate and have more sources of error than oceanic SST retrievals due to the typically larger uncertainties to correct for continental atmospheric air masses, dust and smoke, cloud contamination, water emissivity, and shoreline effects [11,14,15]. Most satellite LSWT retrieval algorithms were designed for ocean surfaces and validated and tuned to oceanic in

situ buoy observations [11,13]. Consequently, the effects of variations in lake elevation, atmospheric profiles of temperature and water vapor, dust and smoke sources, and near-shore pixel contamination by adjacent land surfaces are not typically incorporated in the algorithms when they are applied over inland water bodies. Developing lake-specific algorithms for satellite-derived LSWT is an active area of research and several studies have developed improved techniques for LSWT retrievals [11,15–18]. However, these methodologies have not yet been implemented to our knowledge in a near real-time LSWT analysis.

Representativeness errors may also be introduced when attempting to apply satellite skin surface temperature data to estimate bulk lake temperature [10]. The upper layers of a water column in lakes and oceans are associated with complex variability in temperature. The relationship between bulk temperature measured below the surface by buoys and skin temperature measured by surface radiometers and satellites has been found to be a complex function of atmospheric conditions over lakes [19]. As defined by the Group for High Resolution Sea Surface Temperature (GHRSST, see http://ghrsst-pp.metoffice.com/pages/sst_definitions/), the skin temperature that is measured by satellite radiometers is underlain by “bulk” temperature and “foundation” temperature. Bulk temperature is associated with a transition zone located between the water surface and ~1 m below the surface, where some diurnal cycle in temperature is observed. At a deeper (and variable) depth in the water column, “foundation” temperature, or the temperature where diurnal signals are absent is found. Satellite-derived skin water temperatures can be converted to a “foundation” temperature most readily by utilizing nighttime-only satellite retrievals, where the diurnal variations in the surface water layer due to solar heating are absent and skin effects are more predictable [20].

Extensive gaps in the availability of clear-sky satellite thermal retrievals due to persistent and highly variable seasonal cloud cover over many of the mid-latitude regions of the earth where lakes are abundant makes it difficult to obtain representative LSWT analyses on a daily basis [13,21,22]. Consequently, it is not surprising that the majority of satellite-derived LSWT climatological trend studies have focused on the less-cloudy summer season [22,23]. Over the oceans, gap problems resulting from clouds can be somewhat overcome by the combined use of microwave thermal imagery and in situ buoy data, although sampling uncertainty and errors are noted over some ocean regions [24–26]. The large footprint of satellite microwave temperature retrievals and the impacts of sidelobe contamination within 75 km of shorelines make the data difficult to use over lakes [27]. In addition, most global lakes also lack in situ LSWT observations to supplement satellite analyses.

Cloud masking algorithms have also been shown to struggle over lakes. The algorithms are either too stringent (removing good data in regions of large LSWT gradients), further contributing to the aforementioned gap issues, or insufficient at flagging clouds such as thin cirrus, resulting in cloud contamination in the satellite LSWT retrievals. This is another area of active research, and improved cloud detection techniques have been proposed [28–31].

For the aforementioned and other reasons, it is apparent why it is difficult to provide calibrated long-term spatially- and temporally-consistent LSWT analyses, particularly in near-real time, as lake-specific algorithms are to our knowledge not yet incorporated into operational lake temperature processing schemes [13]. In addition, the only global real-time analyses that currently incorporate the use of higher quality climatological data sets (e.g., the ARC-Lake [15,17,30] and Pathfinder SST climatological datasets for lakes exist for the temporal periods of 1991–2011 and 1985–2014, respectively) for prescribing climatological lake temperature when no actual data coverage exists is the Operational Sea Surface Temperature and Ice Analysis (OSTIA) system, which relaxes to the ARC-Lake climatology in the absence of available data [13].

Despite the difficulties in obtaining accurate LSWT analyses, a number of studies have analyzed historical (and in some cases re-processed) multi-year records of satellite-derived LSWT. This research has shown the importance of lake temperature as one of the key indicators of climate change in lakes, which are known as “sentinels” of climate change [1,32]. A number of studies have analyzed both in situ and long-term available clear-sky satellite LSWT retrievals over the past few decades to better

understand lacustrine response to climate change [18,22,33–37]. These studies have shown that the lake response to climate change is highly variable, even across global sub-regions. Most of these studies used single sensors and single platform types to avoid the issues associated with blending multiple data sets, and therefore mostly limited their analyses to the less-cloudy (and hence less frequent gap periods) warm season.

Many research studies have shown the sensitivity of numerical weather prediction to variations in LSWT, and the value in obtaining reasonably accurate LSWT values for input into these models. LSWT impact many aspects of simulated weather and climate, including global surface temperatures and precipitation [8,9,38–40], and even small lakes typically unresolved in global models impact regional weather [10].

Over the oceans, a number of studies have illustrated the value of combining satellite retrievals from multiple satellite platforms to increase data availability and decrease coverage gaps [41–43]. However, this topic has remained largely unexplored with lakes, with only a few studies suggesting multi-platform data synthesis [13,21,44]. A key need identified by Fiedler et al. [13], is blended near-real time operational analyses of LSWT for input into numerical weather prediction models. Despite the importance of accurate LSWT for input into climate and numerical weather prediction, relatively few studies have been dedicated to improving near-real time LSWT analyses. The Met Office Operational Sea Surface Temperature and Ice Analysis at ~6 km resolution recently included 248 lakes globally [13]. The blended Real Time Global (RTG) dataset at ~8 km resolution is currently used for lake temperature by the National Center for Environmental Prediction [45], but this analysis has been shown to suffer large biases [12]. The resolution (6–8 km) of these analyses is too coarse to resolve thousands of smaller lakes worldwide.

In this paper, we evaluate the current version of the near-real time (~1 day latency) MUR Analysis (<https://mur.jpl.nasa.gov/>) of Lake Surface Temperature from 2007–2015 in a small, medium, and large sized lake. While MUR was designed specifically as a sophisticated high-resolution (~1 km) analysis and blending product for global SST, the MUR global analysis product is also processed daily over thousands of the world's lakes captured by the 1-km nominal MUR resolution. The goal of this study is to determine the feasibility of using the near-real time MUR LSWT analysis for input into numerical weather prediction models, as well as the longer period of record of MUR LSWT (2000–present) for climatological studies. Specifically, this study seeks to determine the quality, strengths, and weaknesses of the current MUR analysis processing applied over inland water bodies, and to provide recommendations for targeted improvements to MUR for future releases with respect to LSWT.

The MUR analysis data and in situ buoy validation sets for the three lakes in this study are described in Section 2. In Section 3, the results of multi-year validations between MUR LSWT analyses and in situ buoy observations for the three lakes are shown, and the ability of the MUR LSWT to capture LSWT variability on daily, weekly, seasonal, and interannual time scales, as well as the strengths and weaknesses of MUR LSWT analyses. In Section 4, conclusions and recommended future improvements to the MUR LSWT are presented.

2. Materials and Methods

2.1. Lakes Analyzed

Satellite-derived MUR LSWT analyses and in situ lake temperature data were analyzed at three lakes (Figure 1). These lakes were chosen to represent variations in lake size. Lake Michigan, bordering Wisconsin, Illinois, Indiana, and Michigan, USA is a large lake 190 km wide and 2600 km long. Lake Okechobee, Florida, USA is a medium-sized lake 48 km wide and 56 km long. Lake Oneida, New York, USA is a relatively small lake 8.0 km wide and 32 km long. The National Oceanic and Atmospheric Administration (NOAA) Great Lakes Environmental Research Laboratory (GLERL) through the CoastWatch program produces a daily near-real time analysis of Lake Michigan temperature named

the Great Lakes Surface Environmental Analysis (GLSEA) [46] (<https://coastwatch.glerl.noaa.gov/>). However, no such operational analyses are produced for Lake Oneida or Lake Okeechobee. These lakes also represent a range of average depth (Lake Michigan, 85.0 m, Lake Okeechobee: 2.7 m; Lake Oneida, 6.7 m) and latitude (Lake Michigan, 44.00°N; Lake Okeechobee: 26.93°N; Lake Oneida, 43.20°N). Lake Michigan partially ices over each winter, and occasionally almost completely freezes over, most recently in 2014. Lake Oneida ice cover is also highly variable, and typically freezes over for at least a month each winter. All three lakes have relatively symmetric shapes and few islands to contaminate the infrared remote sensing retrievals. Lake Michigan and Lake Oneida observe large fractional cloud cover (25–45% according to NCAR regional reanalysis data at <http://www.esrl.noaa.gov/psd/>), and synoptic-scale storms that frequently traverse these regions, which increase the opportunities for LSWT analyses to suffer from data availability loss due to cloud cover reducing the frequency of clear-sky retrievals. The shallow Lake Okeechobee is far enough south that day-to-day air temperature variability is decreased, with fewer synoptic-scale weather systems and less prolonged cloudy periods, both positive factors for obtaining more frequent clear sky retrievals. The seasonal cycles in air temperature and solar forcing are also smaller at Lake Okeechobee than at Lake Michigan and Lake Oneida, resulting in a smaller annual cycle and less interannual variability in lake temperature at Lake Okeechobee than the other two northern lakes.

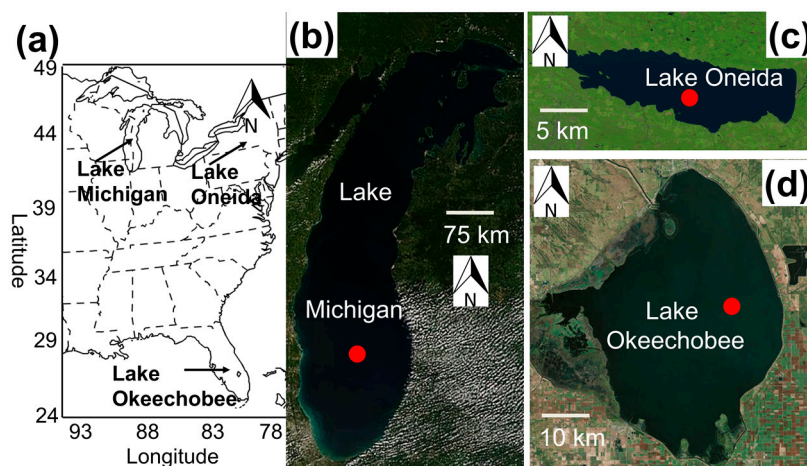


Figure 1. Locations of three USA lakes studied in this paper. (a) overview map; (b–d) Visible satellite images of the lakes; (b) Lake Michigan; (c) Lake Oneida; (d) Lake Okeechobee. In situ buoy location indicated by red dots.

2.2. MUR LSWT Analyses

The National Aeronautics and Space Administration (NASA) Making Earth System Records for Use in Research Environments (MEaSUREs) Multi-scale Ultra-high Resolution (MUR) analysis, hereafter referred to simply as “MUR”, is a global SST analysis field produced daily on a $0.01^\circ \times 0.01^\circ$ grid with an equatorial resolution of 1.1132 km. In addition to coverage over all of the global ocean regions, MUR SST is produced daily over thousands of global inland water surfaces included within the land mask. The MUR SST product has not been previously evaluated or validated for lakes. For the remainder of this document we will refer to MUR SST analysis over inland water bodies as the MUR LSWT. The MUR analysis is described in detail in Chin et al. [43], and only a basic overview is presented here.

MUR LSWT incorporates multiple satellite data sets at different resolutions over multiple time scales within a 5-day window to generate a near real-time analysis (the latency is slightly over a day) that reconstructs small-scale spatial structures of recent and highest resolution satellite-derived LSWT data available while providing the temporal consistency of the data provided over longer time windows by coarser satellite or in situ data. The multi-resolution variational analysis (MRVA) method

(Figure 2) allows data fusion and interpolation using a range of length scales, from 1 km to over 1000 km, specified by a wavelet transform [43].

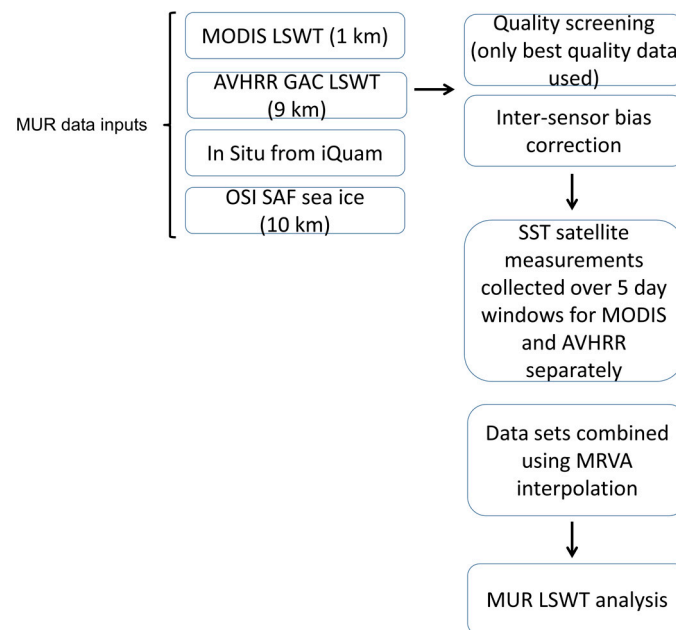


Figure 2. MUR LSWT analysis processing chain.

Over the global oceans, MUR combines over a dozen satellite SST retrievals and buoy near-surface temperature data at different spatial and temporal resolutions over the previous 5 days into a single daily high-resolution SST analysis. Over lakes, only a subset of these data sets is included (Figure 2). MUR provides an estimate of the foundation temperature by utilizing only nighttime satellite data and correcting all retrievals using single sensor error statistics (SSES). MUR utilizes the SSES biases provided with the input data (typically 0.10–0.30 °C) and then these biases are subtracted from the nighttime satellite imagery in MUR to provide a foundation temperature in the final MUR analysis. Inter-sensor bias correction is performed for every data set by MRVA [43]. MUR does not use a background analysis. Therefore, MUR extrapolates SST values from one region to another using the MRVA method when no satellite or in situ observations are available over a given region.

There are several reasons why utilizing nighttime satellite retrievals is preferable. First, nighttime satellite data are typically more easily converted to foundation temperatures, as daytime skin surface and warm layer diurnal heating effects can be up to several °C and highly variable from lake to lake and from day to day, dependent on the lake vertical temperature profile and meteorological conditions such as wind speed [19]. Finally, satellite drift over time could impact the time of day a satellite crosses a lake. Because a lake surface potentially changes more rapidly from one hour of the daytime to the next, the temporal drift in the satellite could potentially introduce sampling errors [22]. By choosing only night data where changes in LSWT vary less over time, these complications are avoided.

Over lakes, MUR combines satellite-derived SST data from thermal infrared sensors on the two primary polar-orbiting satellites that have been historically used for remote sensing of lakes—the Moderate Resolution Thermal Imaging Spectroradiometer (MODIS) and the Advanced Very High Resolution Radiometer (AVHRR) sensors. Available SST samples from microwave sensors tend to be excluded over lakes by MUR due to a stringent threshold on quality flags associated with such samples. The resolution of the MODIS data is approximately 1 km, while the AVHRR data is ~9 km resolution. Thus, the analysis over Lake Oneida incorporates exclusively MODIS data, given the minimum width of the lake is ~8 km (Figure 1). However, both Lake Michigan and Lake Okeechobee are wide enough for both AVHRR and MODIS data to be included in the LSWT analyses. When available, MUR also

incorporates buoy data from the iQuam data network [47]. Over lakes, the only routinely available buoy data in iQuam data network is in the USA Great Lakes, which includes Lake Michigan in this study. No buoy data from Lake Okeechobee or Lake Oneida are included in MUR. In addition to the SST data, MUR also uses an ice fraction ancillary data set at 10 km resolution from the Ocean and Sea Ice Satellite Application Facility (OSI SAF) to help ascertain ice-covered water regions, and parameterizes the temperature as a function of the ice cover [43]. The MUR LSWT analysis for a given day is available a little over a day later. Cloud masking and quality control are applied to the AVHRR and MODIS data sets incorporated into MUR, and only the highest quality possible SST data are used in the MUR LSWT (Figure 2).

For this study, daily subsections of MUR LSWT over each of the three lakes for the 9 year period 2007–2015 were processed and downloaded from the MUR website using OpenDAP <https://mur.jpl.nasa.gov/DownloadDataText.php>.

2.3. In Situ Buoy Data

Buoy and water analyzer data were obtained to validate MUR LSWT over the three lakes in this study for the period 2007–2015. The in situ data were all collected at a depth between 0.05 m and 0.60 m in order to be representative of near-surface temperature. On Lake Michigan, water temperature at 0.6 m depth was measured by a National Oceanic and Atmospheric Administration National Data Buoy Center (NDBC) platform (<http://www.ndbc.noaa.gov/rsa.shtml>). All NDBC buoys go through quality control and calibration procedures as outlined by [48]. On Lake Okeechobee, Water temperature sampling was performed at depth of 0.5 m in the morning with a multi-parameter in situ water analyzer. Water temperature sensors used for Lake Okeechobee were calibrated monthly against the National Bureau of Standards thermometers [49]. On Lake Oneida, near-surface water temperature measurements just below the surface (0.05–0.10 m) were recorded in the morning using Hydrolab Datasonde profilers [50]. For both Lake Okeechobee and Lake Oneida, the measurements were conducted such that minimal disturbance was generated in the water column. However, some mixing of the near-surface lake water is to be expected with such approaches, making it difficult to categorize the representative depth of near-surface LSWT being measured. Additional specifications on these three measurement platforms and sensors are given in Sharma et al. [49].

The buoys or sampling locations were located in deep water and at least several km from the shoreline to avoid land pixel contamination of the satellite retrievals (Figure 1). Only nighttime satellite imagery was used to obtain foundation LSWT and to limit the impacts of solar heating on representativeness errors between the in situ and satellite data. However, some of the diurnal surface heating effects likely impacted the daytime Lake Oneida and Lake Okeechobee in situ measurements (this is a known limitation of these two data sets but no nighttime data was available). Under most conditions, the biases introduced by using daytime bulk lake versus nighttime satellite retrievals are expected to be less than 0.5 °C on average [19], although on calm summer days the differences can be much larger (e.g., see discussion for Lake Michigan in Section 3.5).

The surface water samples from Lake Oneida and Lake Okeechobee in situ data from 2007–2014 were collected weekly for Lake Oneida and bi-weekly to monthly for Lake Okeechobee by boat (data was not collected on Lake Oneida when ice covered the lake). A total of 281 daily matchups between daily MUR LSWT and in situ measurements were conducted for Oneida, and 172 daily matchups between daily MUR LSWT and in situ measurements on Lake Okeechobee. The nearest MUR satellite pixel to the in situ observation location was used for the match-up. On Lake Michigan, nighttime hourly buoy data between 0200 and 0400 Local Standard Time (LST) were compared with the MUR nighttime analyses. A total of 1950 daily matchups between daily MUR LSWT and in situ measurements were conducted on Lake Michigan.

3. Results

3.1. Evaluation Metrics

The evaluation of satellite-derived LSWT retrievals against in situ lake temperature measurements has historically been conducted using two widely used metrics: Root-mean squared error (*RMSE*) and bias. In this study, we also evaluate the ability of the MUR LSWT analysis to capture day-to-day variations in LSWT, as well as to provide cycles of climatological lake temperature. Lakes, being shallower than oceans and surrounded by continental landmasses are typically subject to larger temporal variations in surface temperature. Another important consideration for LSWT analyses is the climatological variability of the LSWT, which varies as a function of latitude, lake depth, and other geophysical forcing mechanisms [17]. For the most part, only the *RMSE* and mean bias of LSWT retrievals has been evaluated in the literature. In this study, we also evaluate the seasonal variations in the satellite-derived LSWT bias and *RMSE*.

Following an overview of the sources of error in the MUR LSWT analyses (Section 3.2), an evaluation of the MUR LSWT for Lake Michigan, Lake Okeechobee, and Lake Oneida is presented using three different criteria. For the first criteria, the standard metrics used in evaluation of SST retrievals of *RMSE* and bias of MUR LSWT analyses versus in situ measurement are evaluated for seasonal and annual time scales (Section 3.3). Second, the ability of the MUR analysis to capture short-term (~few weeks in time, ~10 km in space) spatial and temporal variations in LSWT is evaluated (Sections 3.4 and 3.5). Third, we evaluate the seasonal, interannual, and climatological data from 9 years of daily MUR LSWT analyses (Section 3.6).

3.2. MUR-Specific Sources of Error

LSWT satellite-retrievals are subject to a wide array of potential sources of errors. These include errors associated with the atmospheric correction algorithm as well as a number of other factors (e.g., cloud contamination, shoreline effects, etc.). We refer the reader to Hulley and Hook [11] for an overview of LSWT algorithms, and to Crosman and Horel [14] or Fiedler et al. [13] for an overview of other general error sources in satellite-derived LSWT. In this section, we refer only to MUR LSWT-specific sources of error stemming from the MUR LSWT analysis processing of MODIS and AVHRR satellite imagery. As discussed in Section 2.2, the advantages of the MUR analyses include temporal consistency (available every day), multi-sensor (MODIS and AVHRR) platform data synthesis and bias correction, both high-resolution (MODIS) and medium-resolution (AVHRR) thermal imagery, and sophisticated spatial interpolation and gap filling techniques. However, the current MUR analysis processing techniques can also introduce sources of error and have limitations in addition to the various sources of error typically noted (e.g., cloud contamination, atmospheric correction) in LSWT retrievals. Careful analysis of the MUR LSWT input variables, processing techniques, and final analyses have identified the following potential sources of error in MUR LSWT resulting from the processing methodology:

- Errors introduced by MRVA spatial scale used for interpolating the data as the MRVA system is designed for the open ocean. Analysis values from unrepresentative distant lakes or ocean surfaces may be “spread” to other lake surfaces during periods when no clear-sky retrievals are available over a given lake (Section 3.5).
- Errors resulting from spurious or inaccurate ice cover estimates (i.e., incorrectly specifying open water as ice or vice versa).
- Sampling “gap” errors introduced by only utilizing nighttime satellite imagery, which decreases the frequency of available clear-sky imagery compared to analysis techniques that utilize both daytime and nighttime data.
- Representativeness errors by only utilizing nighttime data. This is not an issue if a daily foundation temperature is deemed to be sufficient for the analysis, which is the current goal of MUR. However,

complications arise on prescribing an appropriate analysis for shallow lakes with climatologically large diurnal temperature ranges through a relatively deep water column.

- Potential under-sampling errors due to the restrictive use of only the data flagged as the highest possible quality in MUR. Some studies have found that the highest quality control consistently throws out large amounts of good data over some lakes [14].

Spurious ice cover in the OSI SAF ice fraction ancillary datasets impacted ~one MUR LSWT analysis time per year on average in Lake Michigan and Oneida, and obviously was not a factor for Lake Okeechobee. An example of effects of the spurious ice cover on a MUR LSWT analysis is shown in Figure 3 for 22 August 2007 (Figure 3).

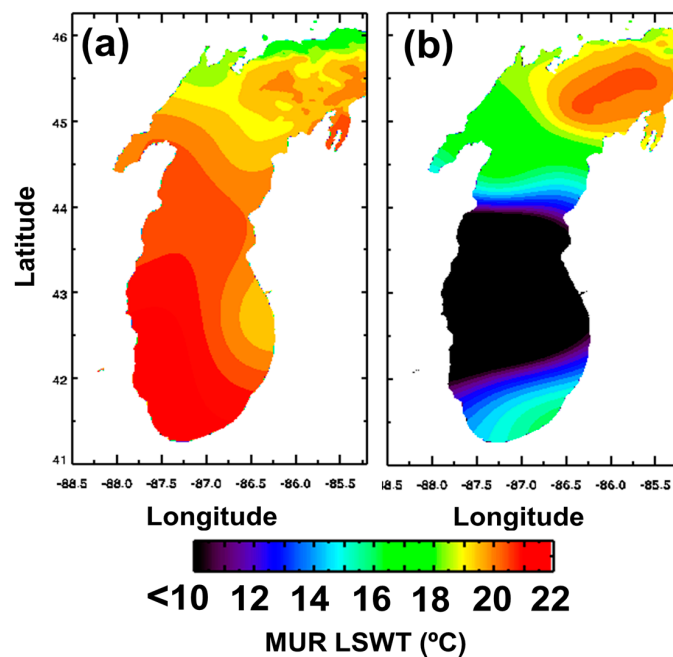


Figure 3. MUR LSWT (°C) analyses on (a) 21 August 2007 and (b) 22 August 2007. Regions colored in black in (b) correspond to temperatures ranging between -4 °C and 10 °C.

Despite the fact that ice cover is not observed over Lake Michigan in August, it is a known problem that spurious ice cover occurs in satellite-derived products over inland lakes due to coastal contamination of microwave imagery used in deriving the mask as the emissivity of the coastline is similar to that of sea ice emissivity [51]. On 21 August 2007, the MUR LSWT analysis agreed well with the in situ buoy observations and provided a realistic spatial map of the temperature variability across Lake Michigan (Figure 3a). There were no ice inputs from the OSI SAF ice fraction data set. However, On 22 August 22, there were 26 false ice inputs that tried to bring the analyzed lake temperature below freezing. These inputs occurred in a region of the lake where no satellite or buoy data was available, thus allowing the false ice to impact the LSWT analysis (Figure 3b). The ice impacts on the MUR LSWT were dramatic and sudden (sudden temperature drops of over 10 °C from one day to the next). These anomalous effects from incorrect ice specification are relatively easy to flag in the data (due to the noted MUR ice input flags and associated unphysical drops in temperature from one day to the next) and are therefore straightforward to quality control and remove. In addition, QC checks to remove spurious ice coverage could be constructed based on climatological checks for spurious ice during historically ice-free months on any given lake. The biases resulting from interpolation of LSWT analysis values from neighboring water bodies were not readily identified, but likely influenced the seasonal variations in MUR versus in situ validation statistics at Lake Oneida, as discussed in Section 3.5.

3.3. In Situ Temperature versus MUR LSWT

In situ buoy temperature measurements taken during the late night (0200–0400 LST) were compared against MUR LSWT (which is an estimate of foundation temperature) at Lake Michigan. The available in situ near-surface water temperatures for Lake Okeechobee and Lake Oneida were only available during the morning hours, and therefore an additional source of uncertainty between the nighttime MUR data and morning in situ observations is introduced. The in situ data was compared to the nearest MUR satellite pixel. MUR defines nighttime as sunset to sunrise, thus any uncertainty introduced in the temporal co-location should be minimized.

The scatter plot of Lake Michigan MUR LSWT versus in situ measurements (Figure 4a) for the period 2007–2015 has an overall cool bias (MUR LSWT-in situ) of -0.20 °C and a *RMSE* of 0.86 °C. Variations are noted in the bias and *RMSE* as a function of season and year (Table 1). On an annual scale, the biases range from -0.41 to 0.47 °C. The bias ranged from -0.02 °C to -0.41 °C during all years but 2014, when surface warming is hypothesized to have warmed the lake surface significantly higher than the buoy water temperature at 0.6 m depth over the summer period (Section 3.5). The annual average *RMSE* also ranged from 0.61 to 1.08 °C on all years except 2014 when it was 1.62 °C (Table 1). Evaluating seasonal averages, the *RMSE* was lowest (0.67 °C) in the fall. This is hypothesized to be due to the weaker stratification of the lake water column during the fall cooling cycle of the lake (warmer water is continually being mixed to the surface as it cools), resulting in less opportunities for representativeness errors between the buoy and satellite observations. Similarly, the higher average *RMSE* of 1.03 during the summer is hypothesized to be due to the high solar insolation effects this time of year and a greater potential for diurnal warming and stratification of the near-surface water column. Evaluation of the time series of plots of annual LSWT also illuminated “lag” errors in the MUR analysis on years with higher *RMSE*. These are errors resulting from the 5-day MUR analysis being unable to respond to rapid atmospheric forcing of surface water temperature. For example, in 2009 the springtime lake temperature warming and fall cooling cycles were accelerated by about 2 weeks each compared to average. In addition, the summertime lake temperatures were more variable on sub-weekly time scales in 2009 than in 2012, which observed the lowest annual *RMSE* during the 2007–2015 period. These factors resulted in increased differences between the MUR analysis and observations during these times when lake temperatures were warming or cooling rapidly, and contributed to the 68% increase in the *RMSE* observed between 2009 versus 2012 for Lake Michigan (Table 1).

Table 1. Comparison of MUR versus in situ LWST data.

Lake Michigan		Bias (MUR LSWT-In Situ, °C)				Root Mean Squared Error (<i>RMSE</i> , °C)			
Year	Spring (MAM)	Summer (JJA)	Fall (SON)	All Months	Spring (MAM)	Summer (JJA)	Fall (SON)	All Months	
2007	-0.07	-0.2	-0.39	-0.24	0.61	1	0.78	0.84	
2008	0.43	0.1	-0.41	-0.02	0.59	0.72	0.71	0.69	
2009	0.14	-0.43	-0.38	-0.29	0.67	1.4	0.7	1.08	
2010	-0.13	-0.56	-0.44	-0.41	0.56	0.76	0.82	0.73	
2011	-0.03	-0.47	-0.23	-0.28	0.77	0.87	0.75	0.8	
2012	-0.09	-0.29	-0.5	-0.32	0.59	0.65	0.68	0.64	
2013	-0.15	-0.27	-0.06	-0.16	0.86	0.68	0.42	0.61	
2014	1.92	0.89	-0.07	0.47	2.52	2.19	0.55	1.62	
2015	NA	-0.79	-0.33	-0.32	NA	1.03	0.7	0.7	
2007–2015	0.25	-0.22	-0.31	-0.2	0.9	1.03	0.67	0.86	
Lake Okeechobee (* Statistics Only Calculated for Sample Size n > 6)									
2007	NA *	NA *	NA *	0.27	NA *	NA *	NA *	0.73	
2008	NA *	NA *	NA *	0.22	NA *	NA *	NA *	0.99	
2009	NA *	NA *	NA *	0.27	NA *	NA *	NA *	0.9	
2010	NA *	NA *	NA *	0.1	NA *	NA *	NA *	1.11	
2011	NA *	NA *	NA *	0.15	NA *	NA *	NA *	0.9	
2012	NA *	NA *	NA *	0.28	NA *	NA *	NA *	1.01	
2013	NA *	NA *	NA *	0.25	NA *	NA *	NA *	0.81	
2014	NA *	NA *	NA *	0.24	NA *	NA *	NA *	0.8	
2007–2014	0.13	-0.13	0.46	0.31	0.69	0.66	1.11	0.91	

Table 1. Cont.

Lake Michigan Year	Bias (MUR LSWT–In Situ, °C)				Root Mean Squared Error (RMSE, °C)			
	Spring (MAM)	Summer (JJA)	Fall (SON)	All Months	Spring (MAM)	Summer (JJA)	Fall (SON)	All Months
Lake Oneida								
2007	–4.25	–2.05	0.02	–1.57	5.79	3.04	1.68	3.46
2008	–4.03	–2.58	0.23	–2.09	4.62	3.43	1.32	3.3
2009	–5.87	–2.59	0.86	–2.8	6.45	3.02	1.29	4.25
2010	–3.55	–2.43	0.75	–1.73	4.13	3.26	1.31	3.12
2011	–3.79	–1.85	0.88	–1.66	5.35	2.55	1.41	3.58
2012	–2.06	–1.27	0.96	–0.86	2.7	1.69	1.51	2.05
2013	–2.86	–1.75	2.05	–0.81	3.63	2.51	2.71	3.07
2014	–5.09	–3.5	0.9	–2.41	5.87	4.61	1.52	4.15
2007–2014	–3.78	–2.65	0.98	–1.74	4.83	3.51	1.78	3.42
2007–2014	March–15 July –3.88	15 July–30 September –0.7	1 October–30 November 1.67		March–15 July 4.71	15 July–30 September 1.13	1 October–30 November 2.23	

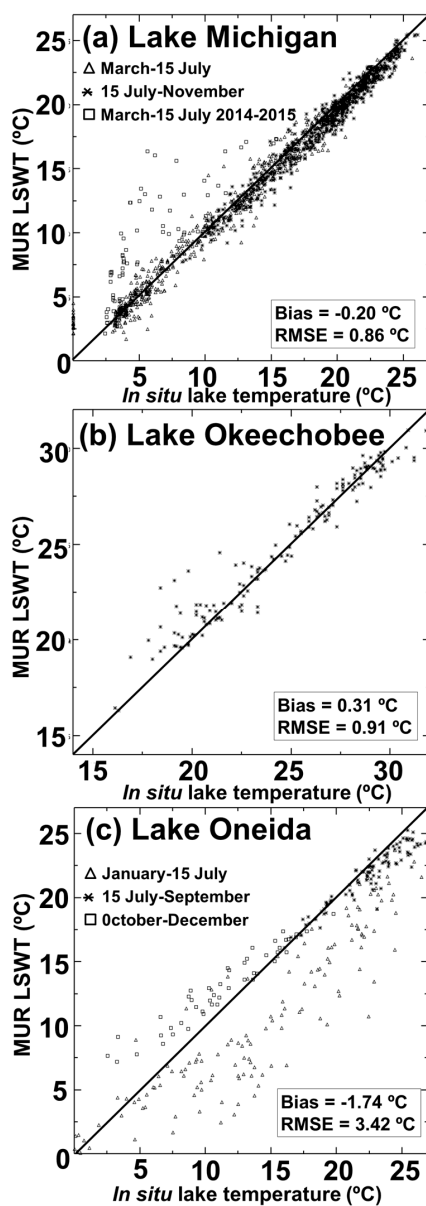


Figure 4. Scatter plots of MUR LSWT analysis versus in situ bulk lake temperature measurements (°C) for period 2007–2015 for (a) Lake Michigan and 2007–2014 for (b) Lake Okeechobee and (c) Lake Oneida. Number of matchups $n = 1950$ for Lake Michigan, $n = 172$ for Lake Okeechobee and $n = 281$ for Lake Oneida.

The scatter plot of Lake Okeechobee MUR LSWT versus in situ measurements for the period 2007–2014 has an overall warm bias of 0.31 °C and a *RMSE* of 0.91 °C (Figure 4b, Table 1). On an annual scale, the biases (*RMSE*) range from 0.10 to 0.28 °C (0.73 to 1.11 °C). The biases and *RMSE* are both decreased on average in the Spring (bias: 0.13, *RMSE* 0.69) and Summer (bias: −0.13, *RMSE* 0.66) compared to the Fall (bias: 0.46, *RMSE* 1.11). The higher bias and *RMSE* in the fall were determined to be impacted by both strong cold fronts impacting the late fall period as well as the more rapid fall cool-down period on Lake Okeechobee compared to a slower spring warm-up (resulting in occasional “lag” temperature errors in the 5-day MUR analysis as discussed earlier).

The scatter plot of Lake Oneida MUR LSWT versus in situ measurements for the period 2007–2014 has an overall cool bias of −1.74 °C and a *RMSE* of 3.42 °C (Figure 4c, Table 1). However, these comparisons show strong seasonality, with a very large cool bias of −3.78 °C and a *RMSE* of 4.83 °C during the spring. During the summer, the bias (*RMSE*) decreases to −2.65 °C (3.51 °C). By fall, the bias (*RMSE*) decreases further to 0.98 °C (1.78 °C). The hypothesized reasons for these strong seasonal discrepancies will be discussed in Section 3.5. Evaluating MUR after the end of periods with large gap errors due to clouds restricting coverage and also potential ice contamination (15 July through September period), decreased the bias further to −0.70 °C and a *RMSE* of 1.13 °C.

3.4. Evaluation of Spatial MUR LSWT

The MUR MRVA interpolation techniques results in LSWT analyses with both temporal consistency, i.e., daily analyses that do not change too abruptly from day to day despite data availability gaps on some days, and realistic spatial structures by combining satellite thermal infrared retrievals of various resolution and frequency (Chin et al. [43]). Despite the lack of microwave imagery, MUR LSWT was able to effectively retain many of the spatial variations in LSWT typically observed in high-resolution analyses of lake temperature such as those observed in the NOAA GLERL GLSEA over Lake Michigan.

Several examples of MUR analyses for 1 July of different years for Lake Michigan and Lake Okeechobee are shown in Figure 5. Realistic spatial variations in LSWT were observed on most days on these lakes (Figure 5a–e). The structures noted in the MUR analyses were evaluated against several NOAA GLERL GLSEA images during an annual cycle. The MUR LSWT patterns in surface temperature generally agreed with the GLSEA (not shown). For example, the 1 July 2010, 2012, and 2016 GLSEA analyses showed similar spatial patterns in LSWT as the MUR analyses shown in Figure 5a–c. Typically, the spatial structures were linked to geophysical forcing, such as variations in the depth of the lake, upwelling, distance to shore, and vertical mixing of the water column. During periods with limited available satellite imagery (generally due to cloud cover), the analyses would revert to a symmetric spatial temperature pattern resulting from the MRVA technique. An example of such a pattern is shown in Figure 5f, with a symmetric gradient in temperature across the water body. This is the result of MRVA “spreading out” the impacts of both coarser resolution thermal imagery and adjacent water bodies during periods when satellite imagery is not available over a lake during the 5-day MUR MRVA analysis window. Further analysis is needed to better quantify both the frequency of occurrence and overall impact of the MRVA interpolation of temperature values between different distinct water bodies separated by land masses in MUR.

On Lake Oneida, the spatial variations in the MUR analyses were small, likely due to the relatively uniform depth of the main body of the lake and the small size of the lake. However, the MRVA technique discussed previously resulted in contamination of LSWT at Lake Oneida by adjacent water bodies (likely Lake Ontario) and introduced large errors in the analyses during Spring and Fall cloudy periods (Section 3.5).

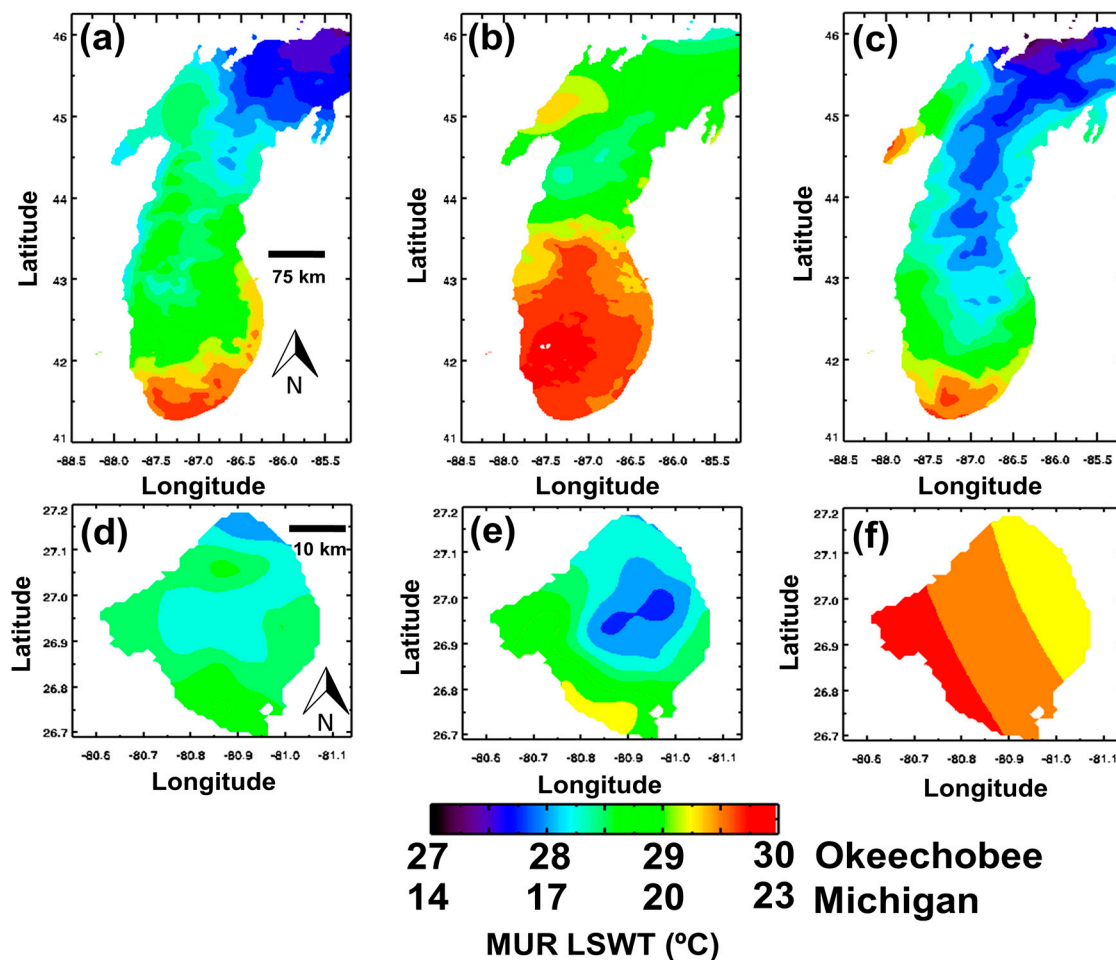


Figure 5. MUR LSWT analyses on 1 July of selected years over (a–c) Lake Michigan and (d–f) Lake Okeechobee. (a) 2010; (b) 2012; (c) 2016; (d) 2007; (e) 2012; (f) 2016.

3.5. Evaluation of Temporal Variability of MUR LSWT

While the validation of in situ versus satellite-derived LSWT “match-ups” of individual thermal images have been conducted for a number of lakes worldwide, none of these studies have analyzed in depth the ability of analyses (such as MUR) that incorporate multi-day satellite retrievals to capture rapid changes in LSWT forced by the overlying meteorology (e.g., summertime surface heating or strong cold fronts). For Lake Michigan, MUR LSWT represents both the rapid spring and summer increase in LSWT and slower fall decreases observed by in situ measurements adequately during all years analyzed with the exception of the Spring 2014 period (Figure 6).

The rapid cool-down associated with cold fronts in September and October 2011 and 2014 were also reflected in the MUR LSWT (Figure 6a,b). In addition, the period of rapid warm-up during June and July 2011 were typically represented by the MUR LSWT analyses for Lake Michigan, with minor lags noted between the in situ and MUR LSWT time series.

The comparisons between MUR LSWT and in situ measurements for Lake Michigan resulted in low biases and *RMSE* on an annual basis (Table 1) except for the May–July 2014 period. During this period, the MUR LSWT versus in situ measurements observed a warm bias of 1.47 °C and a *RMSE* of 2.48 °C (Figure 6b). The large discrepancies between MUR LSWT and in situ buoy data during this period can be ascribed to the following complex factors described below.

An extremely cold winter earlier in 2014 set the stage for unusually high ice coverage on Lake Michigan in early 2014. Consequently, a late ice met resulted in springtime lake temperatures

from March through June that remained unseasonably cool (between 2 °C and 5 °C) (Figure 6b). Consequently, when hot summertime high pressure set up over the Great Lakes region in June and July 2014, large air and water temperature contrasts were observed during this time period, with buoy air temperature 6–18 °C warmer than water temperature at 0.6 m depth (See the arrow corresponding to marker A in Figure 7a,b). Between mid-June and mid-July 2014, Lake Michigan surface temperatures warmed over 15 °C (Figures 6b and 7). This set the stage for multi-day shallow thermoclines or surface warm layers that were modulated by the strength of surface wind speeds, leading to unusually large diurnal swings in lake temperature between 2–6 °C amplitude near the surface of Lake Michigan on days with light winds (Figure 7a,c). The very shallow thermoclines resulted in large temperature differences between the warm skin surface (satellite observation) and cooler sub-surface waters at 0.5–1.0 m depth (buoy observations). For example, between 21 and 27 June 2014, the MUR analysis underestimated LSWT by 2–4 °C (Figure 7a). This period was associated with warm air temperatures and light winds below 3 m s⁻¹ (Figure 7b,c). The LSWT from MUR, even utilizing only nighttime satellite observations, likely were several °C warmer than subsurface buoy temperatures during calm periods. During the period from 29–30 June 2014, the MUR warm bias was decreased to ~1 °C as wind speeds between 5 m s⁻¹ and 10 m s⁻¹ likely mixed out the shallow lake thermocline despite large air-water temperature differences (See the arrow corresponding to marker B in Figure 7a,b). During the period between 8 and 15 July, the buoy lake temperature warmed by 6–7 °C, while the MUR analysis LSWT remained relatively constant (See the arrow corresponding to marker C in Figure 7a,b). During the 9–21 July period, the air-water temperature difference began to decrease, likely as the surface warming of the water column began to penetrate deeper below the surface, and by the 15 July, the MUR LSWT analyses were no longer exhibiting the large warm biases observed previously (Figure 7a).

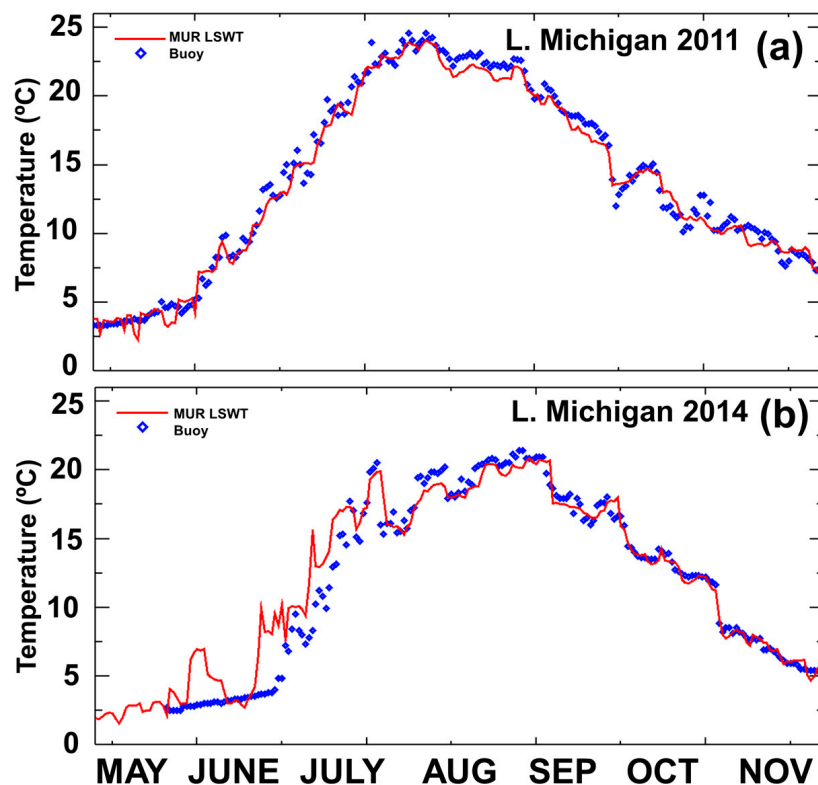


Figure 6. Time series of MUR LSWT analysis compared to in situ measurements for (a) Lake Michigan for 2011 and (b) 2014.

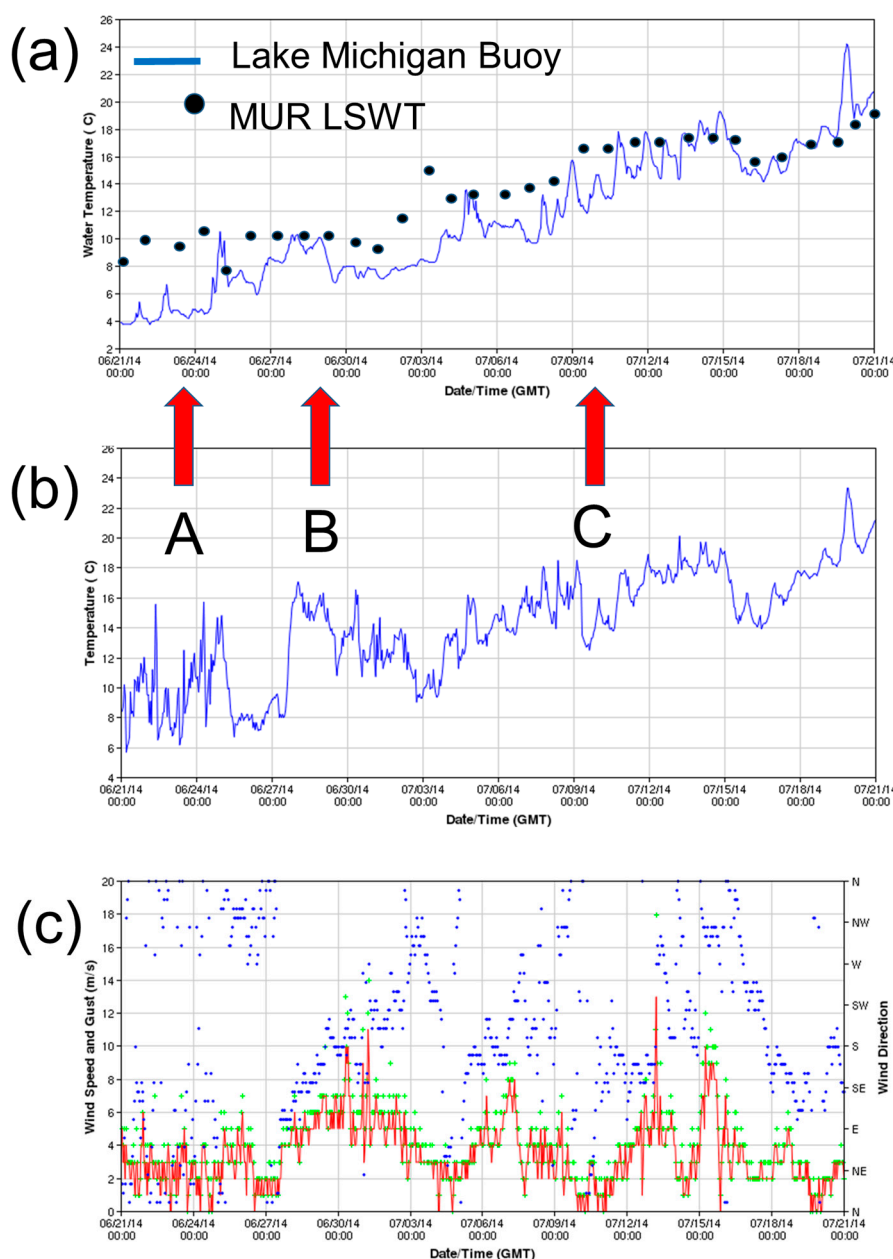


Figure 7. Time series from 21 June 2014 to 21 July 2014 of Lake Michigan buoy (a) water temperature (°C, blue line) (b) air temperature (°C, blue line); and (c) wind speed and direction. Daily MUR LSWT analyses overlaid are indicated by black dots in (a).

At Lake Oneida (Lake Okeechobee), once-per week (1–2 times per month) availability of in situ temperature measurements precludes being able to analyze the ability of MUR LSWT to reproduce day-to-day surface temperature variations. However, the MUR LSWT can be evaluated for Lake Oneida (Lake Okeechobee) on weekly (monthly) to interannual scales (Figure 8).

The Lake Okeechobee MUR LSWT analysis is able to reproduce the annual cycle in LSWT (Figure 8a). While the amplitude of the LSWT cycle is lower at Lake Okeechobee, the highly shallow nature of the lake (2.7 m on average) results in periodic variations in the LSWT analysis throughout the year that are largest in the winter (Figure 8a) when cold fronts have the largest impact on air temperature and the corresponding surface temperature of the shallow lake. In the fall season, the 5-day MUR analysis window also is hypothesized to result in a “lag” effect of the MUR LSWT analysis compared to in situ observations, where cold fronts cool the shallow lake relatively rapidly in a period

of several days. Consequently, in situ observations are typically biased $0.46\text{ }^{\circ}\text{C}$ cooler than MUR LSWT (Figure 8a and Table 1).

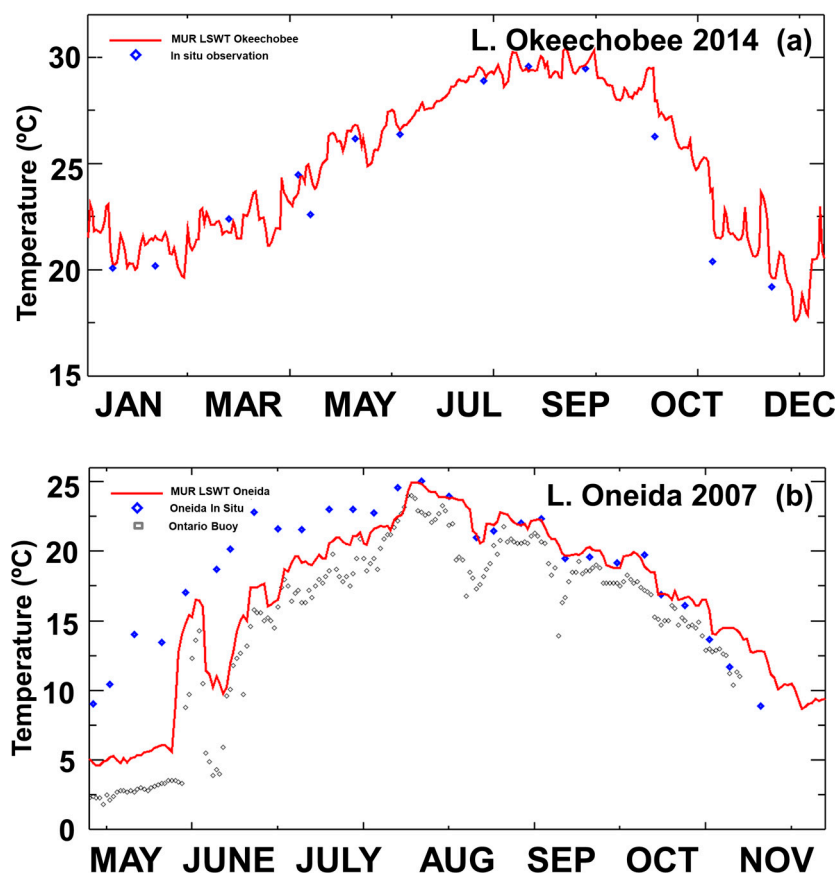


Figure 8. Time series of MUR LSWT analysis compared to in situ measurements for (a) Lake Okeechobee for 2014 and (b) Lake Oneida for 2007. In situ measurements from a Lake Ontario buoy are also included in (b).

The Lake Oneida MUR LSWT analyses are adequate in the mid-July through mid-September period each year, and capture the observed week-to-week variability (Figures 4c and 8b). However, during the spring and fall months, large discrepancies develop between the MUR LSWT and in situ observations. In the spring months, the large errors in the MUR LSWT are believed to be largely due to a lack of available MODIS imagery over the lake due to frequent cloud cover and storms, as well as potential ice contamination. Because of the small dimensions of Lake Oneida (Figure 1), only MODIS imagery is available to the MUR analysis over the lake. During these periods, the thermal infrared retrievals from distant unrepresentative locations (likely Lake Ontario, see how the time series of MUR LSWT for Lake Oneida follows closely in situ buoy measurement from Lake Ontario in both the cloudy spring and fall seasons in Figure 8b) are used by the MUR MRVA technique to “fill in” the data void over Lake Oneida. Because the larger Lake Ontario warms up more slowly than Lake Oneida in the spring, extending these values to Lake Oneida results in the large cool bias of the MUR LSWT versus in situ observations of $-3.88\text{ }^{\circ}\text{C}$ and a *RMSE* of $4.71\text{ }^{\circ}\text{C}$ during the period March through 15 July. During the fall the opposite effect is seen with the larger Lake Ontario cooling off more slowly than Lake Oneida, resulting in the warm bias of the MUR LSWT versus in situ measurements of $0.98\text{ }^{\circ}\text{C}$ (Figure 8b).

3.6. Evaluation of MUR LSWT Interannual Climatology and Trends

The mean annual cycle in MUR LSWT (black dashed lines in Figure 9) varies substantially between Lake Michigan, Lake Oneida, and Lake Okeechobee (note that during the winter months on Lake Michigan and Lake Oneida, the MUR LSWT analyses below 0 °C represent ice surface temperature, not lake temperature). The MUR LSWT ranges from near 0 °C in February and March (as partial ice cover melts) to over 20 °C in the summer on Lake Michigan and Lake Oneida. On Lake Okeechobee, a smaller annual cycle of ~10 °C in MUR LSWT is noted due to the more southern latitude and subtropical climate.

A number of interesting characteristics of the seasonal and interannual variability of LSWT of the three lakes can be seen by analyzing the 9-year climatology (Figure 9).

In Lake Michigan, the large thermal inertia of the large lake results in year-to-year temperature variability. For example, in 2012, an anomalously warm winter with no ice cover, Lake Michigan LSWT was ~5 °C warmer from April through July than in 2014, which was a very cold winter with extensive ice formation on the Lake (Figure 9a). During the cooling phase of the lake from September through December, less interannual variations in LSWT are noted. The warming cycle of LSWT occurs from May through July (~3 months), while the cooling cycle is about 4-month duration (September–December).

On Lake Oneida, the impact of regional weather patterns is evident, with spring to summer 2012 also anomalously warm, and 2014 unusually cold (Figure 9c). Overall, Lake Oneida observes less interannual variations in LSWT compared to Lake Michigan, as the smaller thermal inertia of the lake limits the lag and memory of significant cold and warm spells and winter ice cover on the Lake state (Figure 9c). The cooling cycle during the fall in particular, observed typically small interannual variations in Lake Oneida LSWT.

At Lake Okeechobee, the late fall through early spring months (November–March) observe the greatest interannual variability in LSWT. This is largely the result of more frequent synoptic-scale weather systems penetrating south into Florida during the time period, with cooler surface air temperatures rapidly impacting the shallow lake surface temperature. During the summer months, typically small inter-annual variations in LSWT are noted.

The spatial patterns in LSWT observed by MUR also show interannual variability. For example, the LSWT spatial patterns of Lake Michigan LSWT observed on 1 July 2010, 2012, and 2014 vary as a result of atmospheric forcing and lake state (e.g., ice amount, air temperature). The northern portions of Lake Michigan are deeper and hence typically observe cooler water temperatures through the column, but the impacts of the deep reservoir of cold water are modulated by the amount of vertical mixing of this cooler deep water to the surface.

The impact of the lake bathymetry is seen in the 1 July thermal analyses on 1 July 2010 and 2016 (Figure 5a,c). Interannual variations in the extent and frequency of shallow warming over the Lake during periods of light wind speeds and heat waves, as shown in summer 2012 are also noted (Figure 5b).

Evaluation of the entire period of record of the MUR LSWT (2003–2016) illustrates that given the large inter-annual variability in regional climate, 13 years of data are likely insufficient to describe LSWT trends on these lakes with great confidence, although the climate signals will likely grow as additional years of data are added to the period of record (Figure 10). Analysis of lake spatially varying temperature trends across all three lakes in this study resulted in statistically significant trends in LSWT for each of the lakes between 2003 and 2016. On Lake Michigan, a warming trend of 0.03 °C per year was observed, which is lower than other studies, but likely impacted by the very cold winter in 2014. For Lake Okeechobee, a cooling trend of similar magnitude to the warming at Lake Michigan (−0.03 °C per year) was observed. Lake Oneida observed a weak warming trend of 0.02 °C per year was noted. The observed warming at Lake Oneida and Lake Michigan and observed cooling in the MUR LSWT analyses at Lake Okeechobee agrees broadly with the ARC-Lake climatology 1993–2011 [4].

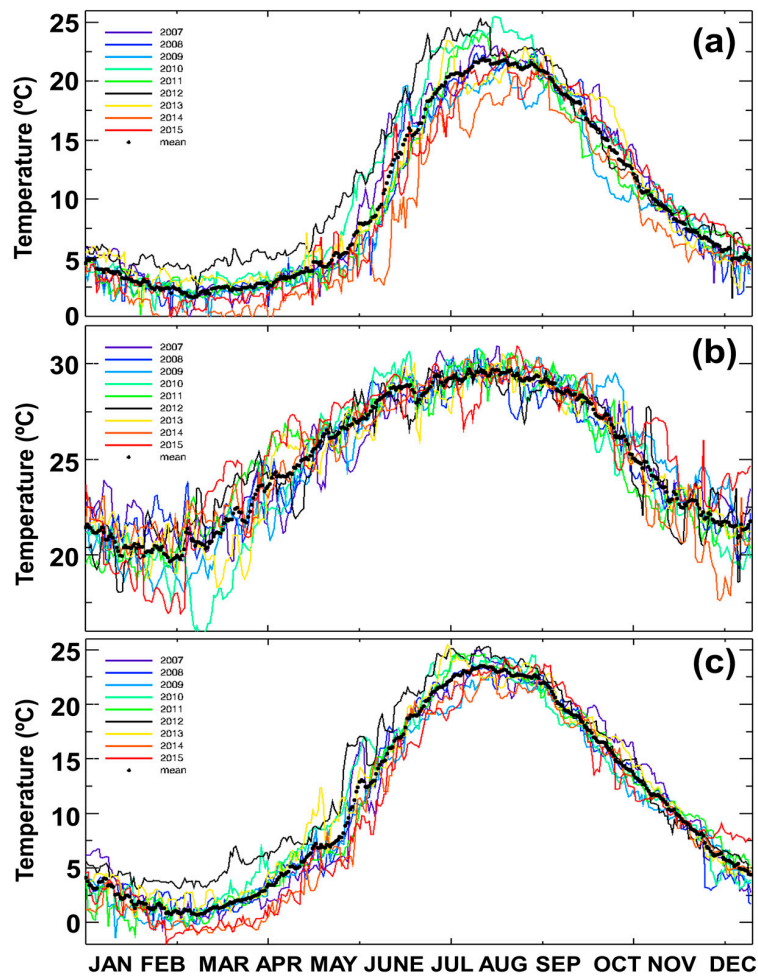


Figure 9. Time series of MUR LSWT analyses (at buoy locations, see Figure 1) for 2007–2015 for (a) Lake Michigan; (b) Lake Okeechobee; (c) Lake Oneida. The dashed thick black line represents the 2007–2015 MUR LSWT mean lake temperature, while individual years are represented by colored lines as indicated in the upper left legend.

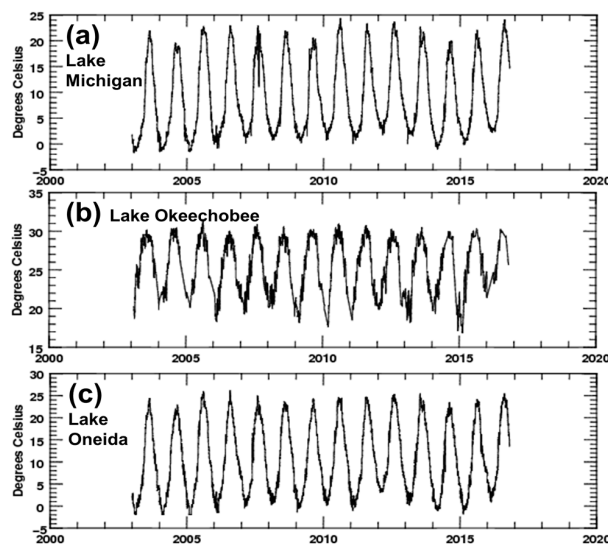


Figure 10. Time series of MUR LSWT 2003–2016 for (a) Lake Michigan; (b) Lake Okeechobee; (c) Lake Oneida.

4. Discussion

The MUR LSWT analyses were compared to buoy temperatures for a small, medium and large lake. The results indicate that the MUR LSWT versus in situ measurements for Lake Michigan (Lake Okeechobee) have an overall bias (MUR LSWT–in situ) of -0.20 °C (0.31 °C) and a *RMSE* of 0.86 °C (0.91 °C). The MUR LSWT versus in situ measurements for Lake Oneida versus in situ measurements have overall large biases (-1.74 °C) and *RMSE* (3.42 °C). For Lake Oneida, problems with spatial interpolation of data from adjacent lakes likely results in large errors in MUR LSWT analyses at this lake for the spring and fall seasons, with much improved analysis during the 15 July–30 September period. The use of daytime in situ validation data at Lake Okeechobee and Lake Oneida compared with nighttime MUR LSWT imagery is a noted limitation of this study, as nighttime bulk lake temperatures at the depth of the buoy observations (less than 1.0 m) are subject to diurnal warming.

The major advantages of the MUR LSWT analyses include daily consistency (analyses generated every day), high resolution (~ 1 km, which provides analyses over many small lakes that are not resolved in coarser analyses), near-real time production (latency of ~ 1 day), and multi-platform data synthesis (MODIS and AVHRR), which increases data availability over the typical single-sensor approach. The high resolution of MUR LSWT allows thousands of lakes to be captured that are not included in other currently available LSWT analyses. The synthesis of multiple years of MUR LSWT to produce a “climatological” LSWT for small lakes not resolved by other products (as well as a higher spatial resolution LSWT data set for larger lakes) is promising for future studies utilizing the MUR LSWT dataset for lakes across the world for a number of potential geophysical applications.

Improved analyses of lake temperature are needed for modeling applications [13]. The results of this study are a promising first step to integrate the MUR LSWT analyses worldwide for providing near-real time lake temperature data for input into geophysical modeling systems. The current MUR LSWT would likely be an improvement over what is currently being used for initializing LSWT in a number of modeling systems, as errors in prescribed LSWT from 3 °C to 10 °C have been noted in currently-used LSWT model analyses [12,52,53].

The results of this study have illuminated a number of error sources that lead us to recommend modifications and future improvements to MUR LSWT. These include:

- Utilize additional high-resolution satellite thermal infrared retrievals over lakes to enhance temporal coverage (e.g., Visible Infrared Imaging Radiometer Suite (VIIRS) onboard the Suomi National Polar-Orbiting Partnership spacecraft [54], as well as the (Sea and Land Surface Temperature Radiometer (SLSTR) onboard the European Space Agency Sentinel-3 fleet of satellites [55], and the GOES-16 Advanced Baseline Imager (ABI) currently onboard the most recently launched National Oceanic and Atmospheric Administration Geostationary Operational Environmental Satellite (GOES-16) [56]. As discussed by Chin et al. [43] plans are already underway to incorporate VIIRS in MUR.
- Potentially incorporate daytime imagery over lakes to increase the amount of available data. MUR already has plans to investigate utilizing daytime imagery when wind speeds are high enough to minimize diurnal warming SST effects [19,20].
- Incorporate lake-specific cloud masking and other quality-control procedures to reduce both contamination and removal of clear-sky imagery.
- Improve ancillary ice cover analyses to reduce spurious unphysical ice coverage impacting LSWT analyses, and develop higher-resolution ice cover analyses to improve coverage for small lakes.
- Reduce the spatial footprint of the MRVA technique to preclude non-representative analysis values from adjacent lakes or oceans to be spread to another lake. Plans to flag input footprints as well as to reduce quality threshold barriers to include microwave LSWT samples are both underway for next version of MUR.

- Determine if a shorter or longer analysis window than the 5 days currently used in MUR would improve the LSWT analyses. Over some lakes where cloud cover is low, a shorter window could allow for a more responsive analysis; over cloudy lakes, a longer window may improve analysis coverage.
- Allow climatological LSWT values derived from the MUR period of record (such as shown in Figure 8) or from external data sets such as ARC-Lake (for lakes >5 km in diameter) to become the default field for MUR LSWT during prolonged cloudy gap periods in lakes with no available in situ observations.

5. Conclusions

This study evaluated MUR LSWT analyses, which are available globally at 1 km resolution, for a small, medium and large lake. The results indicate that the daily near real-time MUR LSWT analyses on annual and seasonal time scales have biases below ± 0.50 °C and RMSE below 1.11 °C for Lake Michigan and Lake Okeechobee, with the exception of 2014 on Lake Michigan (RMSE 1.62 °C) where diurnal thermoclines impacted the representativeness of the buoy measurements. Over small lakes where MODIS is the only current source of data, large errors in the MUR LSWT analyses were noted during periods when cloud cover limits data coverage. However, at this time the MUR LSWT is the only high-resolution near real-time global daily analysis available that resolves thousands of lakes with diameters less than 10 km. We conclude that overall, the MUR LSWT analyses show promise for providing real-time analyses of LSWT for lakes larger than a few km in diameter, but a number of improvements and modifications to MUR are recommended.

Acknowledgments: This research and preparation of this paper was partially supported by Eric Lindstrom, NASA, Multi-sensor Improved Sea Surface Temperature (MISST) for (IOOS), NASA Contract: NNH13CH09C, and also partially funded under a contract with the National Aeronautics and Space Administration (NASA) through the Making Earth System Data Records for Use in Research Environments (MEaSUREs) program. We thank Chelle Gentemann for helping to make this research possible. We thank Lars Rudstam and the Cornell Biological Field Station for providing the temperature data for Lake Oneida, and the National Data Buoy Center for hourly temperature data from Lake Michigan. The South Florida Water Management District provided the water temperature data from Lake Okeechobee. We appreciate the expertise of Robert Grumbine on operational user needs for lake temperature analyses. Nate Larson, Will Howard, Alex Jacques also contributed to this research. Thanks also goes to John Horel for his guidance and advice. We gratefully acknowledge the input of three anonymous reviewers, which significantly improved the paper.

Author Contributions: Erik Crosman, Jorge Vazquez-Cuervo, and Toshio Michael Chin conceived and designed the experiments. Jorge Vazquez-Cuervo and Erik Crosman conducted the validation experiments. Erik Crosman, Jorge Vazquez-Cuervo and Toshio Michael Chin analyzed the data. Erik Crosman wrote the paper.

Conflicts of Interest: The authors declare no conflict of interest.

References

1. Adrian, R.A.; O'Reilly, C.M.; Zagarese, H.; Baines, S.B.; Hessen, D.O.; Wendel, K.; Livingstone, D.M.; Sommaruga, R.; Dietmar, S.; Van Donk, E.; et al. Lakes as sentinels of climate change. *Limnol. Oceanogr.* **2009**, *54*, 2283–2297. [[CrossRef](#)] [[PubMed](#)]
2. MacKay, M.D.; Neale, P.J.; Arp, C.D.; De Senerpont Domis, L.N.; Fang, X.; Gal, G.; Jöhnk, K.D.; Kirillin, G.; Lenters, J.D.; Litchman, E.; et al. Modeling lakes and reservoirs in the climate system. *Limnol. Oceanogr.* **2009**, *54*, 2315–2329. [[CrossRef](#)]
3. Bresciani, M.; Giardino, C.; Boschetti, L. Multi-temporal assessment of bio-physical parameters in lakes Garda and Trasimeno from MODIS and MERIS. *European. Ital. J. Remote Sens.* **2011**, *43*, 49–62.
4. Hook, S.J.; Wilson, R.C.; MacCallum, S.; Merchant, C.J. Lake Surface Temperature [in "State Absolute of the Climate in 2011"]. Available online: <ftp://ftp.ncdc.noaa.gov/pub/data/cmb/bams-sotc/climate-assessment-2011.pdf> (accessed on 10 July 2017).
5. Lenters, J.D.; Hook, S.J.; McIntyre, P.B. Workshop examines warming of lakes worldwide. *Eos Trans. Am. Geophys. Union* **2012**, *93*, 427. [[CrossRef](#)]
6. Lenters, J. The Global Lake Temperature Collaboration (GLTC). *LakeLine* **2015**, *35*, 9–12.

7. Woolway, R.I.; Cinque, K.; de Eyto, E.; DeGasperi, C.; Dokulil, M.; Korhonen, J.; Maberly, S.; Marszelewski, W.; May, L.; Merchant, C.J.; et al. Lake surface temperature [in “State of the climate in 2015”]. *Bull. Am. Meteorol. Soc.* **2016**, *97*, S17–S18.
8. Dutra, E.; Stepanenko, V.M.; Balsamo, G.; Viterbo, P.; Miranda, P.M.A.; Mironov, D.; Schär, C. An offline study of the impact of lakes on the performance of the ECMWF surface scheme. *Boreal Environ. Res.* **2010**, *15*, 100–112.
9. Balsamo, G.; Salgado, R.; Dutra, E.; Boussetta, S.; Stockdale, T.; Potes, M. On the contribution of lakes in predicting near-surface temperature in a global weather forecasting model. *Tellus A* **2012**, *64*, 15829. [[CrossRef](#)]
10. Javaheri, A.; Babbar-Sebens, M.; Miller, R.N. From skin to bulk: An adjustment technique for assimilation of satellite-derived temperature observations in numerical models of small inland water bodies. *Adv. Water Resour.* **2016**, *92*, 284–298. [[CrossRef](#)]
11. Hulley, G.C.; Hook, S.J.; Schneider, P. Optimized split-window coefficients for deriving surface temperatures from inland water bodies. *Remote Sens. Environ.* **2011**, *115*, 3758–3769. [[CrossRef](#)]
12. Grim, J.A.; Knievel, J.C.; Crosman, E.T. Techniques for using MODIS data to remotely sense lake water surface temperatures. *J. Atmos. Ocean. Technol.* **2013**, *30*, 2434–2451. [[CrossRef](#)]
13. Fiedler, E.; Martin, M.; Roberts-Jones, J. An operational analysis of lake surface water temperature. *Tellus A* **2014**, *66*, 21247. [[CrossRef](#)]
14. Crosman, E.T.; Horel, J.D. MODIS-derived surface temperature of the Great Salt Lake. *Remote Sens. Environ.* **2009**, *113*, 73–81. [[CrossRef](#)]
15. MacCallum, S.N.; Merchant, C.J. Surface Water Temperature Observations of large lakes by optimal estimation. *Can. J. Remote Sens.* **2012**, *38*, 25–45. [[CrossRef](#)]
16. Hook, S.J.; Vaughnan, R.G.; Tonooka, H.; Schladow, S.G. Absolute radiometric in-flight validation of mid infrared and thermal infrared data from ASTER and MODIS on the Terra Spacecraft using the Lake Tahoe, CA/NV, USA, automated validation site. *IEEE Trans. Geosci. Remote Sens.* **2007**, *45*, 1798–1807. [[CrossRef](#)]
17. Layden, A.; Merchant, C.; MacCallum, S. Global climatology of surface water temperatures of large lakes by remote sensing. *Int. J. Climatol.* **2015**, *35*, 4464–4479. [[CrossRef](#)]
18. Riffler, M.; Lieberherr, G.; Wunderle, S. Lake surface water temperatures of European Alpine lakes (1989–2013) based on the Advanced Very High Resolution Radiometer (AVHRR) 1 km data set. *Earth Syst. Sci. Data* **2015**, *7*, 1–17. [[CrossRef](#)]
19. Wilson, R.C.; Hook, S.J.; Schneider, P.; Schladow, S.G. Skin and bulk temperature difference at Lake Tahoe: A case study on lake skin effect. *J. Geophys. Res. Atmos.* **2012**, *118*, 10332–10346. [[CrossRef](#)]
20. Donlon, C.; Rayner, N.; Robinson, N.; Poulter, D.J.; Casey, K.S.; Vazquez-Cuervo, J.; Armstrong, E.; Bingham, A.; Arino, O.; Gentemann, C.; et al. The Global Ocean Data Assimilation Experiment HighResolution Sea Surface Temperature Pilot Project. *Bull. Am. Meteorol. Soc.* **2007**, *88*, 1197–1213. [[CrossRef](#)]
21. Oesch, D.C.; Jaquet, J.M.; Klaus, R.; Schenker, P. Multi-scale thermal pattern monitoring of a large lake (Lake Geneva) using a multi-sensor approach. *Int. J. Remote Sens.* **2008**, *29*, 5785–5808.
22. O’Reilly, C.M.; Sharma, S.; Gray, D.K.; Hampton, S.E.; Read, J.S.; Rowley, R.J.; Schneider, P.; Lenters, J.D.; McIntyre, P.B.; Kraemer, B.M.; et al. Rapid and highly variable warming of lake surface waters around the globe. *Geophys. Res. Lett.* **2015**, *42*, 10773–10781. [[CrossRef](#)]
23. Torbick, N.; Ziniti, B.; Wu, S.; Linder, E. Spatiotemporal lake skin summer temperature trends in the Northeastern United States. *Earth Interact.* **2016**, *20*, 1–21. [[CrossRef](#)]
24. Bulgin, C.E.; Embury, O.; Merchant, C.J. Sampling uncertainty in gridded sea surface temperature products and Advanced Very High Resolution Radiometer (AVHRR) Global Area Coverage (GAC) data. *Remote Sens. Environ.* **2016**, *117*, 287–294. [[CrossRef](#)]
25. Castro, S.L.; Wick, G.A.; Steele, M. Validation of satellite sea surface temperature analyses in the Beaufort Sea using UpTempO buoys. *Remote Sens. Environ.* **2016**, *187*, 458–475. [[CrossRef](#)]
26. Liu, Y.; Minnett, P.J. Sampling errors in satellite-derived infrared sea-surface temperatures. Part I: Global and regional MODIS fields. *Remote Sens. Environ.* **2016**, *177*, 48–64. [[CrossRef](#)]
27. Hao, Y.; Cui, T.; Singh, V.P.; Zhang, J.; Yu, R.; Zhang, Z. Validation of MODIS Sea Surface Temperature Product in the Coastal Waters of the Yellow Sea. *IEEE J. Sel. Top. Appl. Earth Obs. Remote Sens.* **2017**, *10*, 1667–1680. [[CrossRef](#)]

28. Merchant, C.J.; Harris, A.R.; Maturi, E.; MacCallum, S. Probabilistic physically-based cloud screening of satellite infra-red imagery for operational sea surface temperature retrieval. *Q. J. R. Meteorol. Soc.* **2005**, *131*, 2735–2755. [[CrossRef](#)]
29. Hulley, G.C. *MODIS Cloud Detection over Large Inland Water Bodies: Algorithm Theoretical Basis Document*; Jet Propulsion Laboratory-California Institute of Technology: Pasadena, CA, USA, 2009.
30. MacCallum, S.N.; Merchant, C.J. *ARC-Lake Algorithm Theoretical Basis Document—ARC-Lake. v1.1, 1995–2009* [Dataset]. The University of Edinburgh, School of GeoSciences/European Space Agency. Available online: <http://hdl.handle.net/10283/88> (accessed on 10 July 2017).
31. Fan, X.; Tang, B.; Wu, H.; Yan, G.; Li, Z. Daytime land surface temperature extraction from MODIS thermal infrared data under cirrus clouds. *Sensors* **2015**, *15*, 9942–9961. [[CrossRef](#)] [[PubMed](#)]
32. Castendyk, D.N.; Obryk, M.K.; Leidman, S.Z.; Gooseff, M.; Hawes, I. Lake Vanda: A sentinel for climate change in the McMurdo Sound Region of Antarctica. *Glob. Planet. Chang.* **2016**, *144*, 213–227. [[CrossRef](#)]
33. Schneider, P.; Hook, S.J. Space observations of inland water bodies show rapid surface warming since 1985. *Geophys. Res. Lett.* **2010**, *37*. [[CrossRef](#)]
34. Politi, E.; Cutler, M.J.; Rowan, J.S. Using the NOAA Advanced Very High Resolution Radiometer to Characterize temporal and spatial trends in water temperature of large European lakes. *Remote Sens. Environ.* **2012**, *126*, 1–11. [[CrossRef](#)]
35. Politi, E.; MacCallum, S.; Cutler, M.E.J.; Merchant, C.J.; Rowan, J.S.; Dawson, T.P. Selection of a network of large lakes and reservoirs suitable for global environmental change analysis using Earth Observation. *Int. J. Remote Sens.* **2016**, *37*, 3042–3060. [[CrossRef](#)]
36. Mason, L.A.; Riseng, C.M.; Gronewold, A.D.; Rutherford, E.S.; Wang, J.; Clites, A.; Smith, S.D.; McIntyre, P.B. Fine-scale spatial variation in ice cover and surface temperature trends across the surface of the Laurentian Great Lakes. *Clim. Chang.* **2016**, *138*, 71–83. [[CrossRef](#)]
37. Moukomla, S.; Blanken, P.D. Remote Sensing of the North American Laurentian Great Lakes' Surface Temperature. *Remote Sens.* **2016**, *8*, 286. [[CrossRef](#)]
38. Zhao, L.; Jin, J.; Wang, S.Y.; Ek, M.B. Integration of remote-sensing data with WRF to improve lake-effect precipitation simulations over the Great Lakes region. *J. Geophys. Res.* **2012**, *117*, D09102. [[CrossRef](#)]
39. Kourzeneva, E. Assimilation of lake water surface temperature observations using an extended Kalman filter. *Tellus A.* **2014**, *66*, 21510. [[CrossRef](#)]
40. Strong, C.; Kochanski, A.K.; Crosman, E.T. A slab model of the Great Salt Lake for regional climate simulation. *J. Adv. Model. Earth Syst.* **2014**, *6*, 602–615. [[CrossRef](#)]
41. Chao, Y.; Li, Z.; Farrara, J.; Hung, P. Blending sea surface temperatures for multiple satellites and in situ observations for coastal oceans. *J. Atmos. Ocean. Technol.* **2009**, *26*, 1415–1426. [[CrossRef](#)]
42. Nardelli, B.B.; Tronconi, C.; Pisano, A.; Santoleri, R. High and ultra-high resolution processing of satellite sea surface temperature data over Southern European Seas in the framework of MyOcean project. *Remote Sens. Environ.* **2013**, *129*, 1–16. [[CrossRef](#)]
43. Chin, T.M.; Vazquez, J.; Armstrong, E.M. A multi-scale high-resolution analysis of global sea surface temperature. *Remote Sens. Environ.* **2017**. in review.
44. Pareeth, S.; Salmaso, N.; Adrian, R.; Neteler, M. Homogenised daily lake surface water temperature data generated from multiple satellite sensors: A long-term case study of a large sub-Alpine lake. *Sci. Rep.* **2016**, *6*, 31251. [[CrossRef](#)] [[PubMed](#)]
45. Thiebaut, J.; Rogers, E.; Wang, W.; Katz, B. A new high resolution blended real-time global sea surface temperature analysis. *Bull. Am. Meteorol. Soc.* **2004**, *84*, 645–656. [[CrossRef](#)]
46. Schwab, D.J.; Leshkevich, G.A.; Muhr, G.C. Automated mapping of surface water temperature in the Great Lakes. *J. Great Lakes Res.* **1999**, *25*, 468–481. [[CrossRef](#)]
47. Xu, F.; Ignatov, A. Error characterization in iQuam SSTs using triple collocations with satellite measurements. *Geophys. Res. Lett.* **2016**, *43*, 10826–10834. [[CrossRef](#)]
48. National Data Buoy Center (NDBC), NDBC Technical Document 09-02: Handbook of Automated Data Quality Control Checks and Procedures. 2009. Available online: <http://www.ndbc.noaa.gov/NDBCHandbookofAutomatedDataQualityControl2009.pdf> (accessed on 27 June 2017).
49. Sharma, S.; Gray, D.K.; Read, J.S.; O'Reilly, C.M.; Schneider, P.; Qudrat, A.; Gries, C.; Stefanoff, S.; Hampton, S.E.; Hook, S.; et al. A global database of lake surface temperatures collected by in situ and satellite methods from 1985–2009. *Sci. Data* **2015**, *2*, 150008. [[CrossRef](#)] [[PubMed](#)]

50. Rudstam, L.G. Limnological Data and Depth Profile from Oneida Lake, New York, 1975-Present. Web Data on Knowledge Network for Biocomplexity, 2015. Available online: <http://knb.ecoinformatics.org/#view/kgordon.35.70> (accessed on 26 June 2017).
51. Lavergne, T.; Tonboe, R.; Lavelle, J.; Eastwood, S. Algorithm Theoretical Basis Document for the OSI SAF Global Sea Ice Concentration Climate Data Record. 2016. Available online: https://www.researchgate.net/profile/Thomas_Lavergne3/publication/306365213_Algorithm_Theoretical_Basis_Document_ATBD_for_the_OSI_SAF_Global_Sea_Ice_Concentration_Climate_Data_Record_v11/links/57baff8108ae202e6a579100.pdf (accessed on 20 June 2017).
52. Blaylock, B.K.; Horel, J.D.; Crosman, E.T. Impact of a lake breeze on summer ozone concentrations in the Salt Lake Valley. *J. Appl. Meteorol. Climatol.* **2017**, *56*, 353–370. [[CrossRef](#)]
53. Spero, T.L.; Nolte, C.G.; Bowden, J.H.; Mallard, M.S.; Herwehe, J.A. The impact of incongruous lake temperature on regional climate extremes downscales from the CMIP5 archive using the WRF model. *J. Clim.* **2016**, *29*, 839–853. [[CrossRef](#)]
54. Hillger, D.; Kopp, T.; Lee, T.; Lindsey, D.; Seaman, C.; Miller, S.; Solbrig, J.; Kidder, S.; Bachmeier, S.; Jasmin, T.; Rink, T. First-light imagery from Suomi NPP VIIRS. *Bull. Am. Meteorol. Soc.* **2013**, *94*, 1019–1029. [[CrossRef](#)]
55. Donlon, C.; Berruti, B.; Buongiorno, A.; Ferreira, M.H.; Féménias, P.; Frerick, J.; Goryl, P.; Klein, U.; Laur, H.; Mavrocordatos, C.; et al. The global monitoring for environment and security (GMES) sentinel-3 mission. *Remote Sens. Environ.* **2012**, *120*, 37–57. [[CrossRef](#)]
56. Schmit, T.J.; Griffith, P.; Gunshor, M.M.; Daniels, J.M.; Goodman, S.J.; Lebar, W.J. A Closer Look at the ABI on the GOES-R Series. *Bull. Am. Meteorol. Soc.* **2017**, *98*, 681–698. [[CrossRef](#)]



© 2017 by the authors. Licensee MDPI, Basel, Switzerland. This article is an open access article distributed under the terms and conditions of the Creative Commons Attribution (CC BY) license (<http://creativecommons.org/licenses/by/4.0/>).